Journal of Engineering Research and Reports

22(8): 1-20, 2022; Article no.JERR.86652
ISSN: 2582-2926

Empirical Modeling and Optimization of Base Activated Ngbo Catalysts in Esterification Reaction Using Response Surface Methodology

V. N. Nwobasi [a*], Philomena K. Igbokwe [b] and Akindele Oyetunde Okewale [c]

[a] Department of Food Science and Technology, EBSU, Abakaliki, Nigeria.
[b] Department of Chemical Engineering, UNIZIK, Awka, Nigeria.
[c] Department of Chemical Engineering, Federal University of Petroleum Resources, Effurun, Delta State, Nigeria.

Authors' contributions

This work was carried out in collaboration among all authors. All authors read and approved the final manuscript.

Article Information

DOI: 10.9734/JERR/2022/v22i817550

Open Peer Review History:
This journal follows the Advanced Open Peer Review policy. Identity of the Reviewers, Editor(s) and additional Reviewers, peer review comments, different versions of the manuscript, comments of the editors, etc are available here: https://www.sdiarticle5.com/review-history/86652

Original Research Article

Received 02 March 2022
Accepted 04 May 2022
Published 23 May 2022

ABSTRACT

In this work, Box-Behnken's Response Surface Methodology (RSM) was applied to study the esterification reaction effectiveness of base-activated Ngbo clay catalyst. The esterification was monitored based on temperature, time duration, amount of reactant, catalyst weight, and particle size. The Box-Behnken's Response Surface Methodology indicates that the base clay-catalyzed esterification reactions proceed through dual Acid-complex and Alcohol-complex mechanisms, with the alcohol mechanism dominating. The acetic acid and ethanol esterification efficiencies by base-activated Ngbo clay catalyst optimized using RSM models indicated the esterification percentage was >99%. The predicted and experimental values under the same conditions showed less than 5% difference, thereby making the Box-Behnken design approach an efficient, effective, and reliable method for the esterification of acetic acid with ethanol. The produced catalyst was optimized using A-One way ANOVA modelled, which indicated that the correlation coefficient of the regression was 0.9940. The result implied that 99.40% of the total variation in the esterification reaction was due to the experimental

**Corresponding author: Email: nwobasiveronica@yahoo.com;*

variables. The obtained data in this study indicated that this process could be applied in the esterification of acetic acid to avoid the drawbacks of corrosion, loss of catalyst, and environmental problems.

Keywords: Optimization; characterization; esterification; base activated clay catalyst; response surface methodology; Box-Behnken design.

1. INTRODUCTION

There is increased research on the development of solid acid catalysts for esterifications, adsorption of contaminants in wastewater, and other various organic transformations. Even though there are sets of regulations established to aid in the substitution of unfriendly and corrosive liquids used in chemical and petrochemical industries, the use of solid acid catalysts for esterifications and adsorption of water contaminants is essential [1,2].

Esterification reactions have long been carried out in a homogeneous phase in acid catalysts such as sulphuric acid, hydrochloric acid, and p – toluene sulfonic acid (p – TSOH), which have drawbacks of corrosion, loss of catalyst, and environmental problems [3,4]. Therefore, research has been focused on developing eco-friendly heterogeneous catalysts to synthesize fatty acid esters. The most popular solid acids catalyst used to produce esters were ion-exchange organic resins, such as Amberlyst – 15 [5,6], Zeolites [7,8,9], and Silica-supported heteropoly acid [10] and [11]. Nevertheless, they have shown limitations in the applicability for modelled esterification reaction due to low thermal stability (Amberlyst-15 < 140^{o}C), mass transfer resistance (Zeolites) [12,13], or loss of active acid sites in the presence of a polar medium (HPA/silica) [11].

Clay is one of the raw materials in abundance in Nigeria. It is readily available in Nigeria in large deposits, yet its potential has not been fully explored. However, there is recent interest in exploring the possibility of clays, such as the bleaching of palm oil [14,15], in adsorption of dyes [16–18], among others. In a quest to develop green processes, clay is mainly used to synthesize catalysts. However, Nigerian clays from Ningbo, Ohaukwu- Ebonyi State, for producing clay catalysts are limited in the literature. However, the kinetics of clay-catalyzed esterification reactions is abundant in literature but with little or no data on the mechanistic and empirical 2models2 of the use of Ngbo clay.

Response Surface Methodology (RSM) collects statistical and mathematical techniques that use quantitative data. Central composite design (CCD), Box-Behnken, and Doehlert designs (BBD) are the principal response surface methodologies used in experimental design. This method is suitable for fitting a quadratic surface. It helps optimize the effective parameters with a minimum number of experiments and analyzes the interaction between the parameters [6]. The objective is to optimize a response (output variable) influenced by several independent variables (input variables). The application of RSM to design optimization aims to reduce the cost of numerous expensive experiments, save time, reduce stress, etc. [19–22].

This work investigated the use of local clay from Ngbo in Ohaukwu Local Government Area of Ebonyi State, Nigeria, to produce a base-activated catalyst and optimize the clay catalyst's effectiveness for the esterification acetic acid with ethanol using Response Surface Methodology.

2. MATERIALS AND METHODS

2.1 Source of Raw Materials

The clay sample was obtained from Ngbo in Ohaukwu L.G.A. of Ebonyi State (N 06^{o}30' 32.8''), (E 007^{o}58'13.7''). The dye was purchased from a chemical shop at Ogbete main market, Enugu, Enugu State. Other chemicals such as conc. Sodium hydroxide, distilled water, etc., were all of the standard grades.

2.2 Physico-Chemical Characterization of Ngbo Clay

The Ngbo clay sample was subjected to physical analysis to obtain their physical properties. The analysis carried out includes: Bulk density, Moisture content, pH, and Loss of Ignition (LOI).

2.3 Characterization of the Raw Clay and Base Activated Sample

The Ngbo clay sample was characterized using XRF and XRD.

2.4 Base Activation

The base activation method used in this work is reported by [23]. A 100g of pulverized and screened clay was mixed into a slurry with 50ml of diluted water, and 30ml of 1M NaOH was added and stirred vigorously and placed in an oven where it was maintained at a temperature of 100^{o}C. The sample was washed after that and left to sediment. Complete removal of all residual bases was achieved by repeating washing and decanting until a pH of six was obtained. The final slurry was filtered and dried at 100^{o}C. The dried, activated, and washed clay was then pulverized, screened and stored in desiccators prior to use.

2.5 Optimization of Process Conditions on the Catalyst Quality Produced Using Esterification Process

2.5.1 Sample preparation/procedure

The raw clay sample was crushed and sieved at 100 microns, 200 microns, and 300 microns. After that, the clay sample was activated using the base (NaOH) method. The base-activated clay sample was used in the esterification reaction to assess the effectiveness. The predetermined weight of the clay sample was weighed; one mole of ethanol and acetic acid was each modeled into the clay sample to ensure that the ethanol did not block the active sites of the catalyst. The container was tightly closed; the contents were shaken vigorously and immersed in a water bath shaker maintained at the experimental design conditions in Table 1. The summary of the reaction equation is:

$$CH_3COOH + C_2H_5OH \rightleftharpoons CH_3COOC_2H_5 + H_2O \quad (1)$$

On titration, the equation becomes:

$$CH_3COOH + NaOH \longrightarrow CH_3COONa + H_2O \quad (2)$$

Table 1. The natural and coded values of the independent variables used

Variables	Natural values			Coded values		
	Low level	Mid-point	High level	Low level	Mid Point	High level
Temperature (^{o}C), A	50	70	90	-1	0	+1
Process duration (minutes), B	30	195	360	-1	0	+1
Excess reactant (ml), C	2.5	3.75	5	-1	0	+1
Catalyst weight (grammes), D	0.25	0.38	0.5	-1	0	+1
Particle size (microns), E	100	200	300	-1	0	+1

The clay-catalyzed esterification was 3modeled using Box-Behnken Response Surface Methodology.

For five factors inputs of x_1, x_2, x_3, x_4, and x_5, the equation of the quadratic response is given as;

$$Y = b_o + b_1X_1 + b_2X_2 + b_3X_3 + b_4X_4 + b_5X_5 + b_{12}X_1X_2 + b_{13}X_1X_3 + b_{14}X_1X_4 + b_{15}X_1X_5 + b_{23}X_2X_3 + b_{24}X_2X_4 + b_{25}X_2X_5 + b_{34}X_3X_4 + b_{35}X_3X_5 + b_{45}X_4X_5 + b_{11}X_1^2 + b_{22}X_2^2 + b_{33}X_3^2 + b_{44}X_4^2 + b_{55}X_5^2. \quad (3)$$

2.6 Response Surface Methodology

The response surface technique applying the Box-Behnken design matrix was used to study the interaction and effects among the factors and their level of contribution and significance in the clay-

catalyzed esterification. This method determines the needed best working conditions in a shorter time and provides detailed processes conditions. This was achieved through a designed experimental design applying the Box-Behnken Response Surface Methodology design of 46 steps of an experiment consisting of five factors and three levels (Table 2). The numerical optimization method of RSM was used in the optimization.

Table 2. Box-Benhken's response surface methodology design of experiment

Std	Run	Factor A (°C)	Factor B (min)	Factor C (ml)	Factor D(g)	Factor E (mic)
37	1	70	30	3.75	0.25	200
22	2	70	360	2.5	0.38	200
23	3	70	30	5	0.38	200
29	4	70	195	2.5	0.38	100
26	5	90	195	3.75	0.25	200
1	6	50	30	3.75	0.38	200
32	7	70	195	5	0.38	300
46	8	70	195	3.75	0.38	200
10	9	70	360	3.75	0.38	100
34	10	90	195	3.75	0.38	100
21	11	70	30	2.5	0.38	200
35	12	50	195	3.75	0.38	300
8	13	70	195	5	0.5	200
4	14	90	360	3.75	0.38	200
2	15	90	30	3.75	0.38	200
11	16	70	30	3.75	0.38	300
31	17	70	195	2.5	0.38	300
3	18	50	360	3.75	0.38	200
24	19	70	360	5	0.38	200
16	20	90	195	5	0.38	200
44	21	70	195	3.75	0.38	200
12	22	70	360	3.75	0.38	300
36	23	90	195	3.75	0.38	300
17	24	70	195	3.75	0.25	100
18	25	70	195	3.75	0.5	100
45	26	70	195	3.75	0.38	200
33	27	50	195	3.75	0.38	100
25	28	50	195	3.75	0.25	200
20	29	70	195	3.75	0.5	300
27	30	50	195	3.75	0.5	200
30	31	70	195	5	0.38	100
42	32	70	195	3.75	0.38	200
41	33	70	195	3.75	0.38	200
39	34	70	30	3.75	0.5	200
6	35	70	195	5	0.25	200
43	36	70	195	3.75	0.38	200
38	37	70	360	3.75	0.25	200
19	38	70	195	3.75	0.25	300
40	39	70	360	3.75	0.5	200
7	40	70	195	2.5	0.5	200
28	41	90	195	3.75	0.5	200
14	42	90	195	2.5	0.38	200
5	43	70	195	2.5	0.25	200
13	44	50	195	2.5	0.38	200
9	45	70	30	3.75	0.38	100
15	46	50	195	5	0.38	200

3. RESULTS AND DISCUSSION

3.1 Physical Properties of the Raw Clay

The result of the physical properties of raw Ngbo clay is presented in Table 3. The result showed that the clay has a moisture content of 3.3 % and bulk density of 1.25 g/ml, which is in agreement with the previous research [24–26] that reported the moisture content of kaolinite clay is between 3.0 – 4.0%, and the bulk density is 1.2 – 1.4 g/ml.

3.2 Characterization of Raw Clay and Base Activated Clay

The chemical properties of the raw Ngbo clay were analyzed using XRF and XRD.

The XRF composition analysis of raw Ngbo clay and Base activated Ngbo clays (BAC) results are presented in Table 4. The result showed that raw and activated clays have oxides and other impurities contaminations. Still, the clay minerals compositions are not meaningfully affected by base treatments even under strong conditions and below 500℃, as reported by [27,28] and [29]. This shows that improvement on the properties of the clay by chemical methods below 500℃ is difficult due to its low reactivity. This result of the XRF on the Ngbo raw clay and base-activated Ngbo clays, as shown in Table 4, also indicates a high content of silicon and aluminum oxides compared to other oxides.

The results of the XRD pattern analysis of raw Ngbo clay are presented in Fig. 1. The XRD pattern results showed several characteristic peaks due to mineral compositions present. The peak obtained at a position corresponding to 2Θ = 22.64° indicated the presence of large quantities of quartz. Minor impurities, such as illite, muscovite, haloysite, quartz hydrated mica, non-cryistalline hydroxide iron, and halloysite, are present. The presence of these minor impurities and quartz content of Ngbo clay needs to be reduced to a minimum before its usage for industrial purposes, especially in catalysts development in line with [30 and 31] research. The XRD analysis corroborates the results obtained with the XRF analysis.

Table 3. Results of Bulk density, Moisture content, pH, and LOI

Clay type	Bulk density (g/ml)	% moisture content	pH	LOI (%)
Ngbo clay	1.25	3.33	7.5	10.52

Table 4. Results of XRF analysis of raw Ngbo clay and acid-activated Ngbo clay

Chemical constituent	Raw clay (Wt. %)	Base activated (BAC), (Wt. %)
SiO_2	62.70	73.100
TiO_2	1.52	1.468
Al_2O_3	19.70	18.155
Fe_2O_3	2.06	4.521
P_2O_3	_	0.167
CaO	0.789	0.479
MgO	0.026	0.490
Na_2O	0.20	0.101
K_2O	0.85	0.943
Mn_2O_3	_	0.208
V_2O_5	0.071	_
Cr_2O_3	0.035	0.006
CuO	0.044	_
BaO	0.19	_
L.O.I	11.82	_
SO_3	_	0.329
Cl	_	0.017
ZnO	_	0.011
SrO	_	0.007

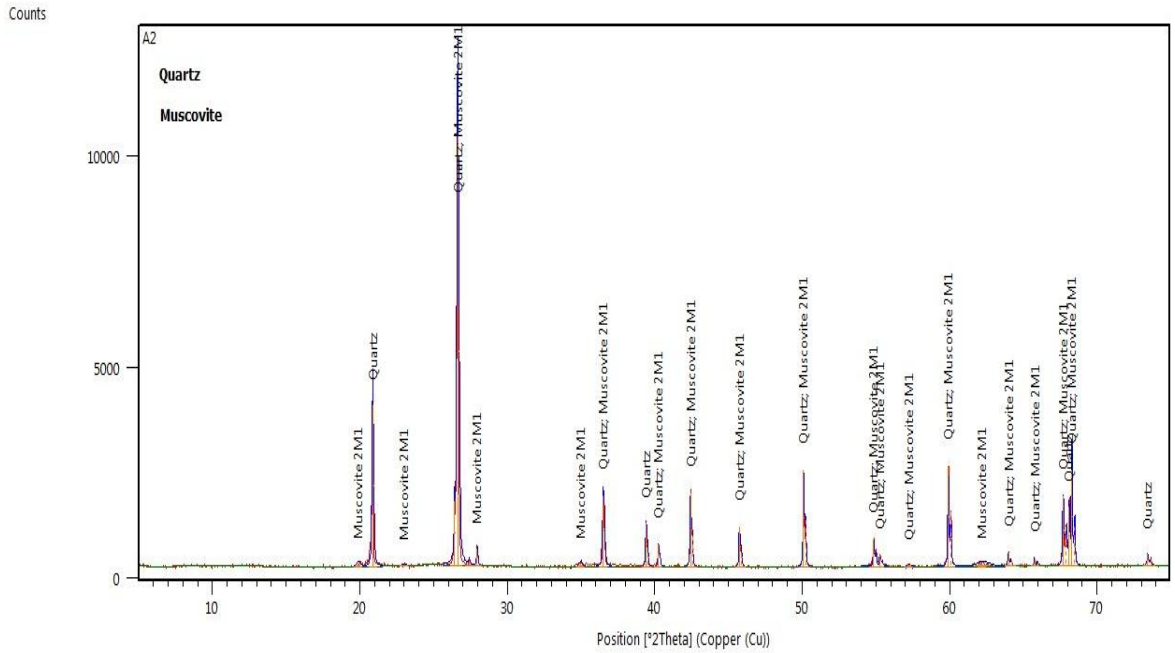

Fig. 1. Results of XRD analysis of base activated clay

The results of XRD pattern analysis of Ngbo base activated clay; BAC is presented in Fig. 1. The XRD pattern results showed several characteristic peaks due to mineral compositions present. The analysis of the peaks showed sharp peaks with low intensity at $2\theta = 11.30^0$This is the main peak used in identifying kaolinte clay, as reported in the literature by [32].

3.3 Esterification Process Results

The esterification technique was used to obtain the responses and yield of Base Activated Catalyst (BAC), as shown in Table 5.

3.4 Analysis of Variance (ANOVA) for BAC

The ANOVA result of BAC is shown in Table 6. The ANOVA results show that the regression model is highly significant, as evident from the calculated F-value (207.52) and a very low probability value (P =0.0001). The lack of fit F-value of 2.50 implies that it was not significant relative to the pure error, and there is a 15.67% chance that a "Lack of Fit" F-value this large could occur due to noise. All the terms in the regression models are not equally important.

The significant terms of the model were determined by F- value and P- values. The F – value is the mean square of regression (MRR) ratio to the error (MRe). The larger the magnitude of the F – value, the smaller the p-value and the more significant is the corresponding parameter in the regression model [33].

Values of ''Prob > F'' less than 0.0500 indicate that the model terms are significant, while values greater than 0.100 indicate insignificant model terms. ANOVA involves subdividing the total variation of a data set into parts. If the P-value of lack of fit is less than 0.05, there is a statistically significant lack of fit at a 95% confidence level [34]. Table 6 indicates that the significant model terms are A, B, C, E, AB, AC, BC, CE, $B^{2,}$ and E^2. This implies that linear effects of temperature, process duration, amount of reactant, particle size, interactive effects of temperature and process duration, temperature and amount of reactant, process duration and amount of reactant, amount of reactant and particle size, and quadratic effects of process duration and particle size were significant. Other effects included in the model were used to support the hierarchy.

Table 5. Results showing responses and yield of BAC

Std	Run	Factor 1A (°C)	Factor 2B (min)	Factor 3C (ml)	Factor 4D(g)	Factor 5E (mic)	Response (ml)	Yield (%)
37	1	70	30	3.75	0.25	200	32.70	26.68
22	2	70	360	2.5	0.38	200	19.00	57.40
23	3	70	30	5	0.38	200	41.70	6.50
29	4	70	195	2.5	0.38	100	18.50	56.37
26	5	90	195	3.75	0.25	200	28.00	37.22
1	6	50	30	3.75	0.38	200	31.00	30.49
32	7	70	195	5	0.38	300	37.50	12.79
46	8	70	195	3.75	0.38	200	29.00	34.98
10	9	70	360	3.75	0.38	100	27.10	36.08
34	10	90	195	3.75	0.38	100	28.00	33.96
21	11	70	30	2.5	0.38	200	22.00	50.67
35	12	50	195	3.75	0.38	300	30.00	30.23
8	13	70	195	5	0.5	200	38.00	14.80
4	14	90	360	3.75	0.38	200	24.60	44.84
2	15	90	30	3.75	0.38	200	32.40	27.35
11	16	70	30	3.75	0.38	300	32.10	25.35
31	17	70	195	2.5	0.38	300	20.00	53.49
3	18	50	360	3.75	0.38	200	29.70	33.41
24	19	70	360	5	0.38	200	36.00	19.28
16	20	90	195	5	0.38	200	36.30	18.61
44	21	70	195	3.75	0.38	200	28.80	35.43
12	22	70	360	3.75	0.38	300	27.60	35.81
36	23	90	195	3.75	0.38	300	28.00	34.88
17	24	70	195	3.75	0.25	100	29.90	29.48
18	25	70	195	3.75	0.5	100	29.30	30.90
45	26	70	195	3.75	0.38	200	29.10	34.75
33	27	50	195	3.75	0.38	100	32.00	24.53
25	28	50	195	3.75	0.25	200	31.20	30.04
20	29	70	195	3.75	0.5	300	29.00	32.56
27	30	50	195	3.75	0.5	200	31.70	28.92
30	31	70	195	5	0.38	100	38.50	9.20
42	32	70	195	3.75	0.38	200	29.50	33.86
41	33	70	195	3.75	0.38	200	28.40	36.32
39	34	70	30	3.75	0.5	200	32.00	28.25
6	35	70	195	5	0.25	200	38.40	13.90
43	36	70	195	3.75	0.38	200	29.50	33.86
38	37	70	360	3.75	0.25	200	28.00	37.22
19	38	70	195	3.75	0.25	300	29.50	31.40
40	39	70	360	3.75	0.5	200	28.10	37.00
7	40	70	195	2.5	0.5	200	19.50	56.28
28	41	90	195	3.75	0.5	200	28.80	35.43
14	42	90	195	2.5	0.38	200	18.00	59.64
5	43	70	195	2.5	0.25	200	19.40	56.50
13	44	50	195	2.5	0.38	200	20.50	54.04
9	45	70	30	3.75	0.38	100	32.40	23.58
15	46	50	195	5	0.38	200	42.00	5.83

The quality of the model developed was evaluated based on the correlation coefficient, R^2 value. A developed model should be best at low standard deviation and high R2 statistics, closer to unity. It will give a predicted value closer to the actual value for the response (Ahmad et al., 2009). The model accuracy was confirmed by the regression model's correlation coefficient, which is 0.9940. The correlation coefficient showed that 99.40% of the total variation in the final concentration was attributed to the experimental variables considered in this research work. The

high value of the R^2 showed that the predicted value would be more accurate and closer to its actual value [33,35]. The standard deviation for the model was 1.41, which indicated that the predicted values for this model are still considered suitable to correlate with the experimental data. The adequate precision which measured the signal-to-noise ratio was 56.041, which indicated a sufficient signal. Also, the "Pred R-squared" of 0.9774 was in reasonable agreement with the "Adj R-squared" of 0.9892 as reported in the literature by [33,35].

Final equation in terms of coded factors gives:

$$Yield = + 34.87 + 3.40A + 5.14B – 21.47C + 0.11D + 0.78E + 3.64AB + 1.79AC – 0.17 AD – 1.19AE + 1.51BC – 0.45BD – 0.51BE + 0.28CD + 1.62CE – 0.065DE – 0.63A^2 – 1.42B^2 + 0.70C^2 – 0.86D^2 – 3.03E^2. \quad (4)$$

The coefficient with one factor represents the effect of the particular factor. In contrast, the coefficients with two factors and those with second-order terms represent the interaction between two factors and quadratic effect, respectively [33].

Final model equation after eliminating the insignificant terms in terms of coded variables:

$$Yield = + 34.87 + 3.40A + 5.14B – 21.47C + 0.78E + 3.64AB +1.79AC +1.51BC + 1.62CE – 1.42B^2 – 3.03E^2. \quad (5)$$

Table 6. ANOVA Table for BAC

Source	Sum of Squares	df	Mean Square	F - Value	P – Value Prob > F
Model	8194.88	20	409.74	207.52	< 0.0001 significant
A - Temperature	185.23	1	185.23	93.81	< 0.0001
B – Process duration	421.99	1	421.99	213.73	< 0.0001
C – Excess reactant	7373.66	1	7373.66	3734.54	< 0.0001
D – Effect of Catalyst	0.18	1	0.18	0.091	0.7648
E – Particle size	9.63	1	9.63	4.88	0.0366
AB	53.07	1	53.07	26.88	< 0.0001
AC	12.89	1	12.89	6.53	0.0171
AD	0.11	1	0.11	0.057	0.8135
AE	5.71	1	5.71	2.89	0.1014
BC	9.15	1	9.15	4.63	0.0412
BD	0.80	1	0.80	0.41	0.5300
BE	1.04	1	1.04	0.53	0.4746
CD	0.31	1	0.31	0.16	0.6936
CE	10.47	1	10.47	5.30	0.0299
DE	0.017	1	0.017	8.559E-003	0.9270
A^2	3.42	1	3.42	1.73	0.2003
B^2	17.55	1	17.55	8.89	0.0063
C^2	4.25	1	4.25	2.15	0.1549
D^2	6.49	1	6.49	3.29	0.0819
E^2	79.94	1	79.94	40.49	<0.0001
Residual	49.36	25	1.97		
Lack of fit	44.88	20	2.24	2.50	0.1567 not significant
Pure Error	4.48	5	0.90		
Cor Total	8244.24	45			

The regression model developed was further assessed using residual plots. Residual is the difference between the experimental value and the value predicted by the model. Some of the residual plots used were: a plot of residuals vs. predicted values which tests the assumption of constant variance of the experimental data, a plot of residuals vs. run, which checks for lurking variables that may have influenced the response during the experiment, the normal plot of residuals which indicates whether the residuals follow a normal distribution, and plot of predicted vs. Actual response values which helps to detect a value, group of values that the model does not easily predict.

3.4.1 Residual plots for BAC

Figs. 3–5 showed the plots of predicted vs. Actual response values. The plots indicate values that the model does not easily predict. The plot of residuals against run checks for lurking variables that may have influenced the response during the experiment. The normal plot of residuals indicates whether the residuals follow a normal distribution, and the plot of predicted against actual response values helps to detect a value, group of values that the model does not easily predict from the Fig. 2 below, the trends of the residual plots showed that the model could be easily obtained.

3.4.2 Contour plots for BAC

The contour plots were depicted in Figs. 3 to 24. The circular nature of the contour plots signifies that the interactive effects between the variables are not significant, and the optimum values of the test process variables cannot be easily obtained [36]. The non-circular nature of the contour plots reveals an interaction between the process variables studied, and the optimum value of the process variables can be easily obtained.

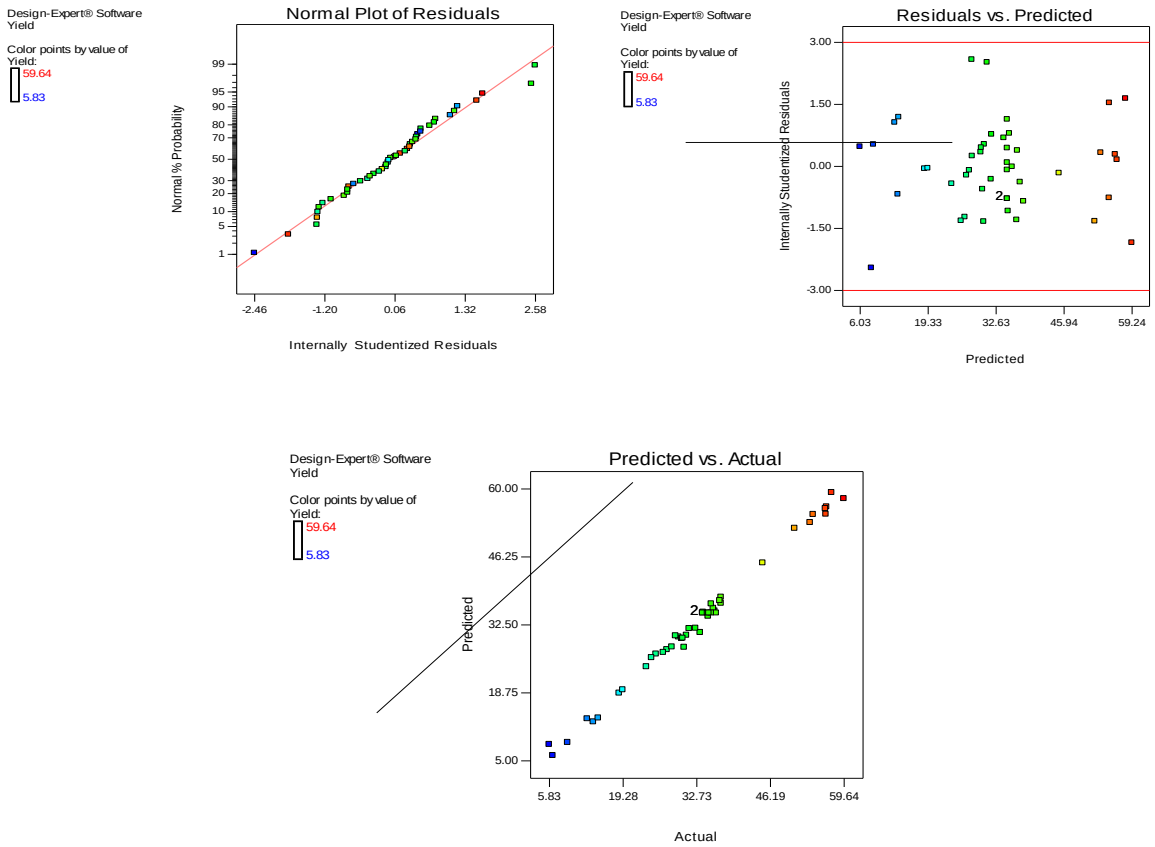

Fig. 2. Normal plot of residual for BAC, the plot of Residual verse predicted for BAC and Plot of predicted verse actual for BAC

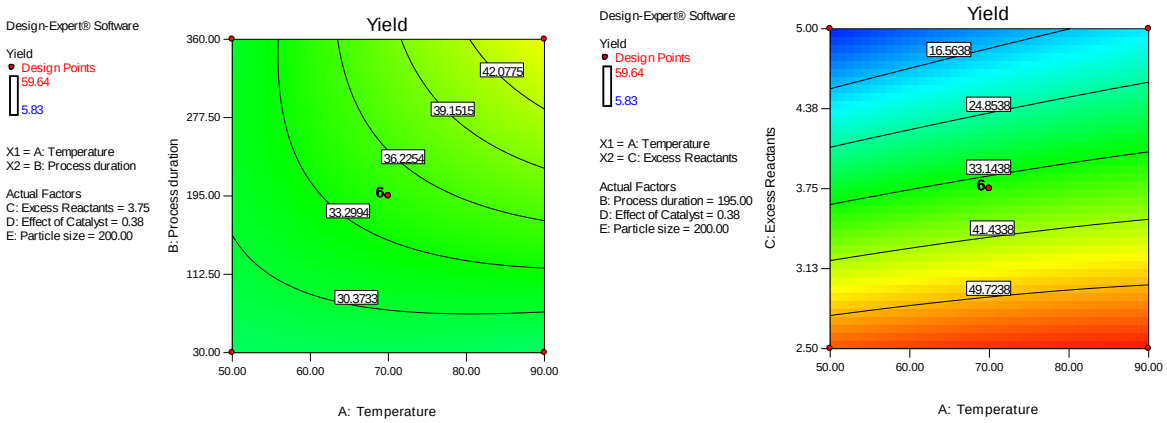

Fig. 3. The contour plots for process duration against temperature and yield of BAC and The contour plots for excess reactants against temperature and yield of BAC

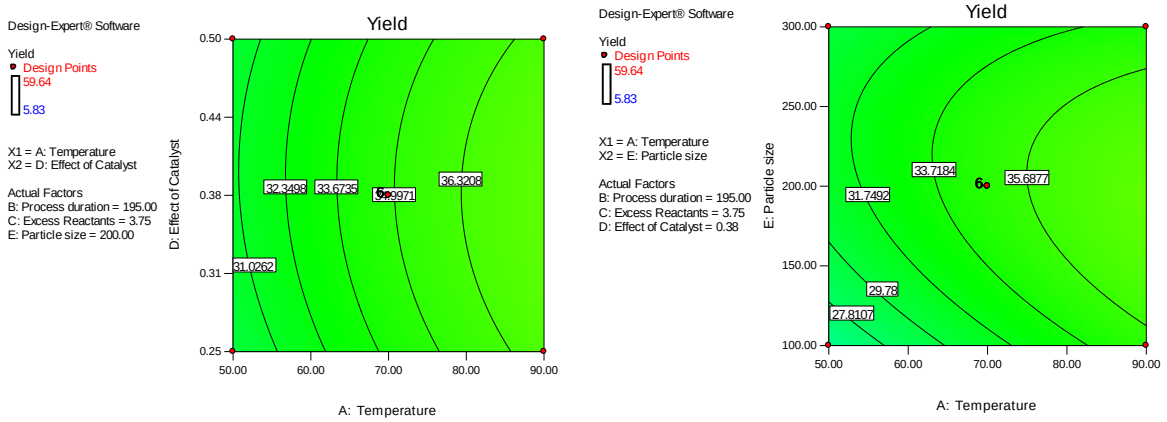

Fig. 4. The contour plots for the effect of catalyst against temperature and yield of BAC and The contour plots for particle size against temperature and yield of BAC

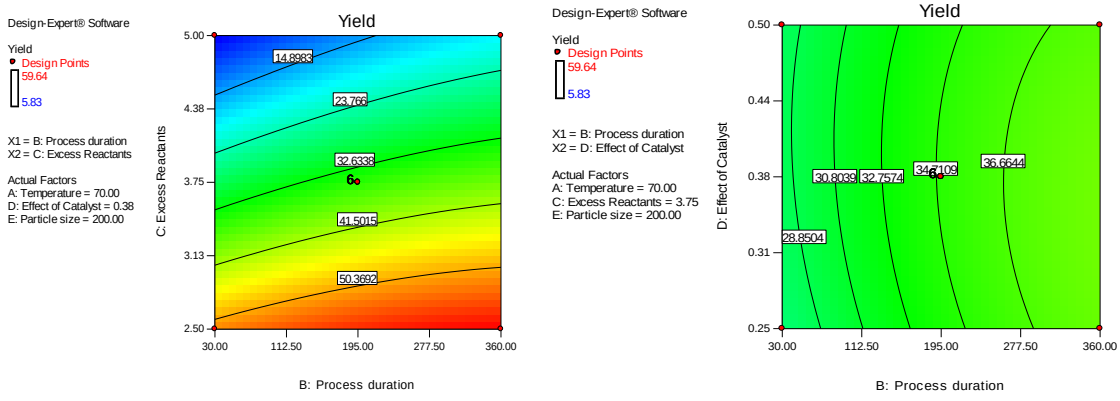

Fig. 5. The contour plots for excess reactants against process duration and yield of BAC and contour plots for the effect of catalyst against process duration and yield of BAC

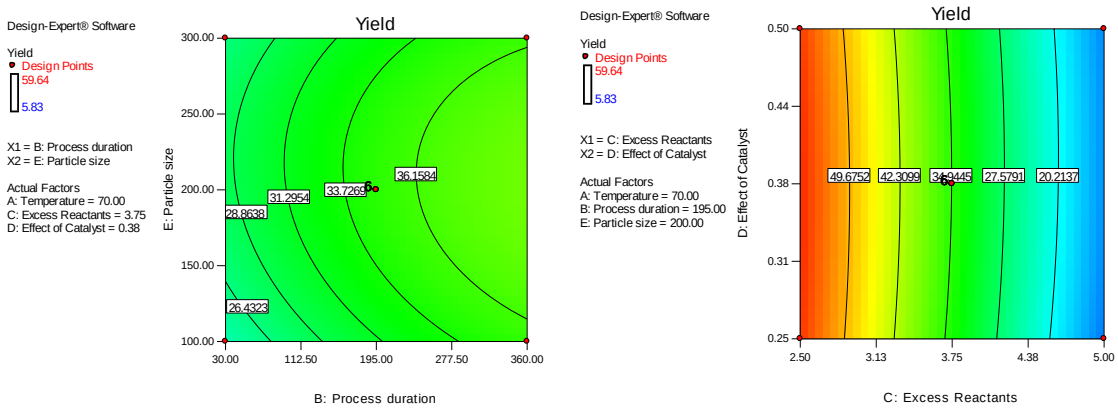

Fig. 6. The contour plots for particle size against process duration and yield of BAC and the contour plots for the effect of catalyst against excess reactant and yield of BAC

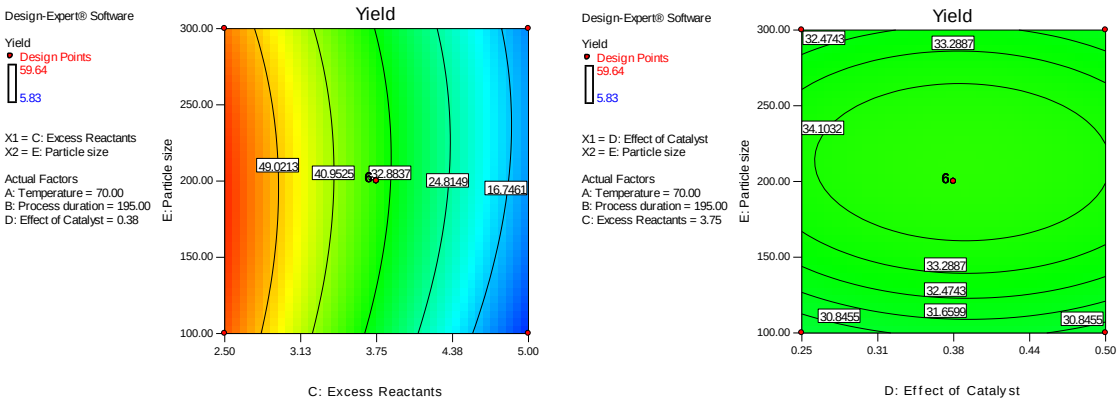

Fig. 7. The contour plots for particle size against excess reactant and yield of BAC and the contour plots for the effect of catalyst against excess reactant and yield of BAC

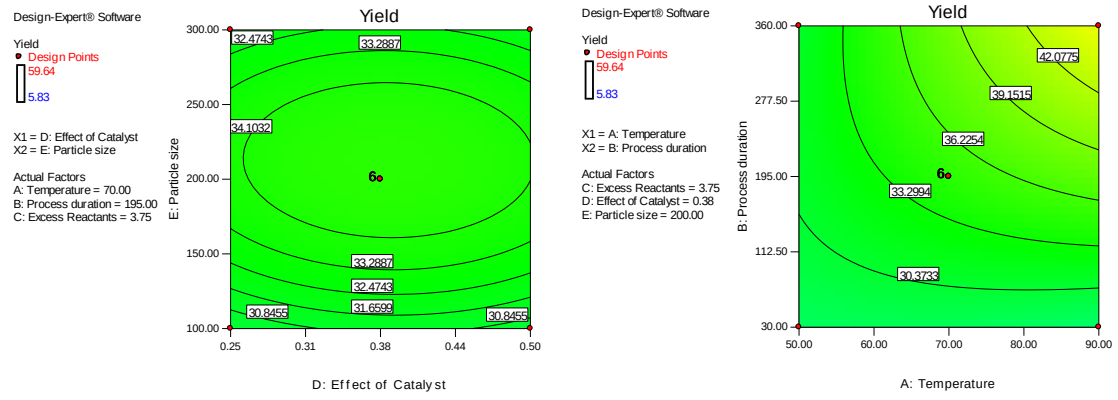

Fig. 8. The contour plots for particle size against the effect of catalyst and yield of BAC and the contour plots for process duration against temperature and yield of BAC

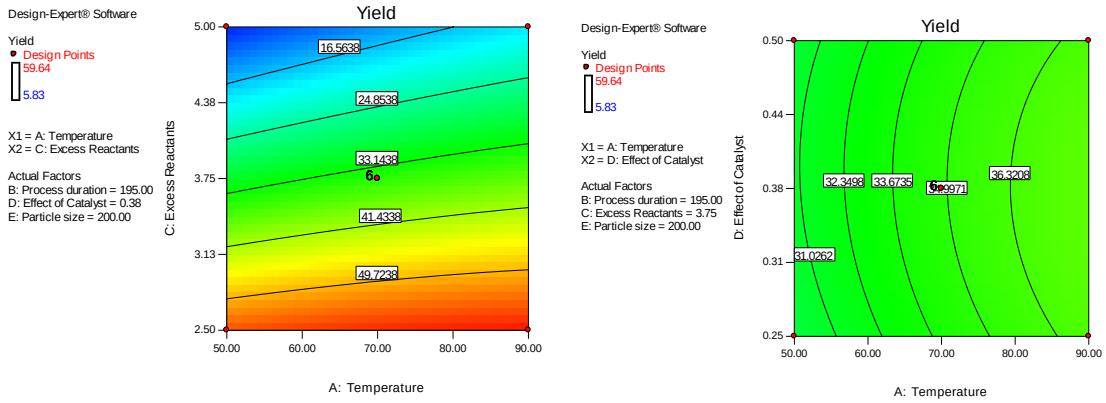

Fig. 9. The contour plots for excess reactants against temperature and yield of BAC and the contour plots for the effect of catalyst against temperature and yield of BAC

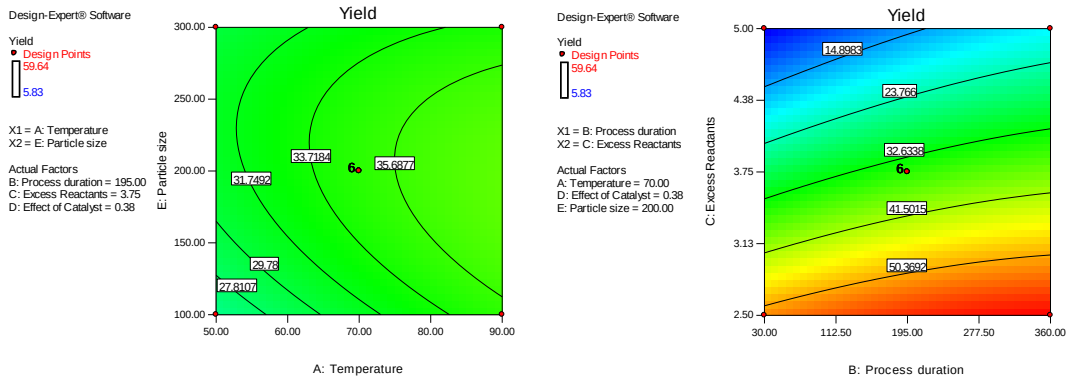

Fig. 10. The contour plots for particle size against temperature and yield of BAC and the contour plots for excess reactant against process duration and yield of BAC

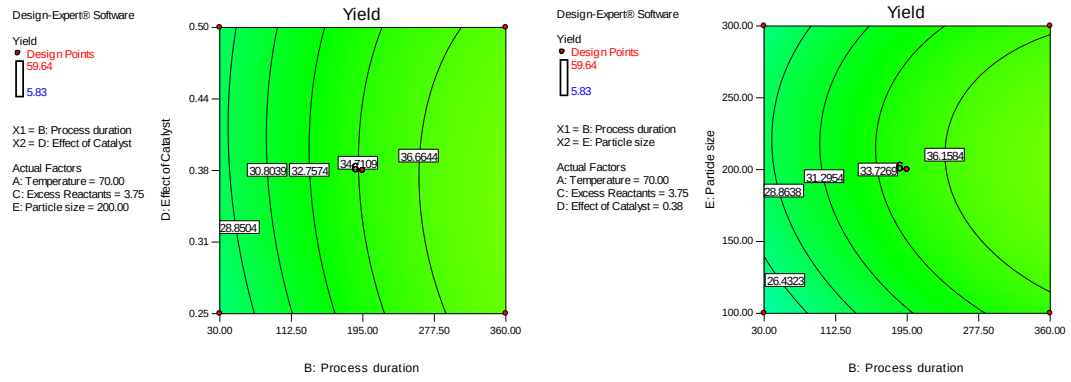

Fig. 11. The contour plots for the effect of catalysts against process duration and yield of BAC and The contour plots for particle size against process duration and yield of BAC

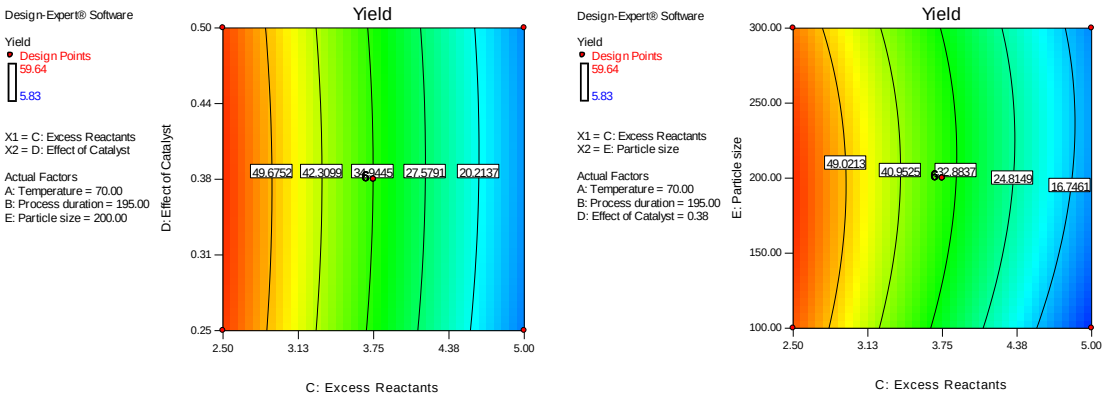

Fig. 12. The contour plots for the effect of catalysts against excess reactants and yield of BAC and The contour plots for the effect of catalysts against excess reactants and yield of BAC

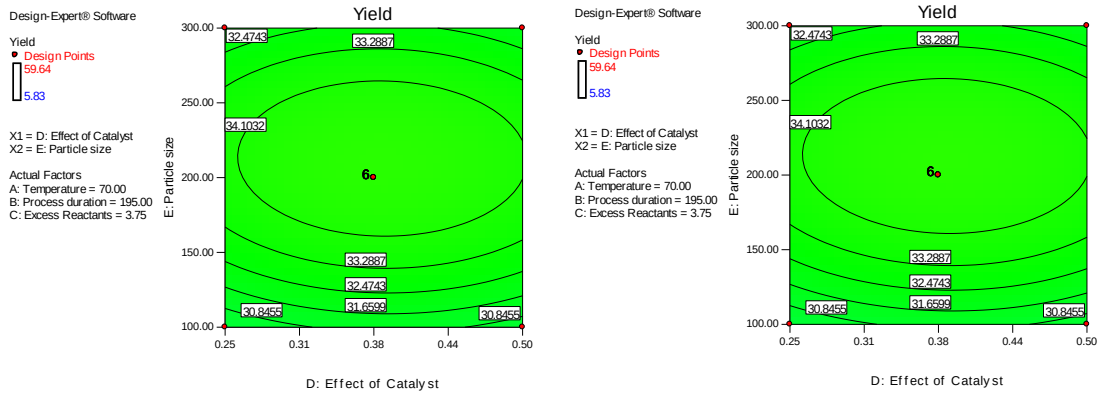

Fig. 13. The contour plots for particle size against excess reactants and yield of BAC and the contour plots for particle size against the effect of catalyst and yield of BAC

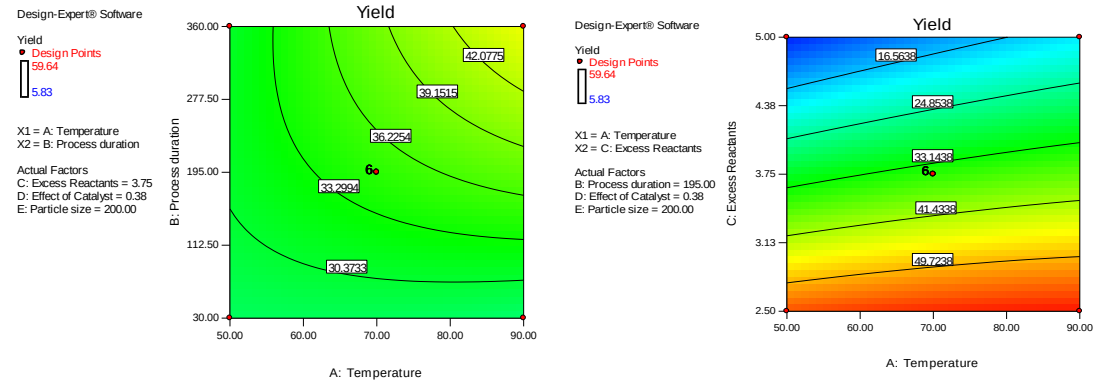

Fig. 14. The contour plots for process duration against temperature and yield of BAC and the contour plots for excess reactants against temperature and yield of BAC

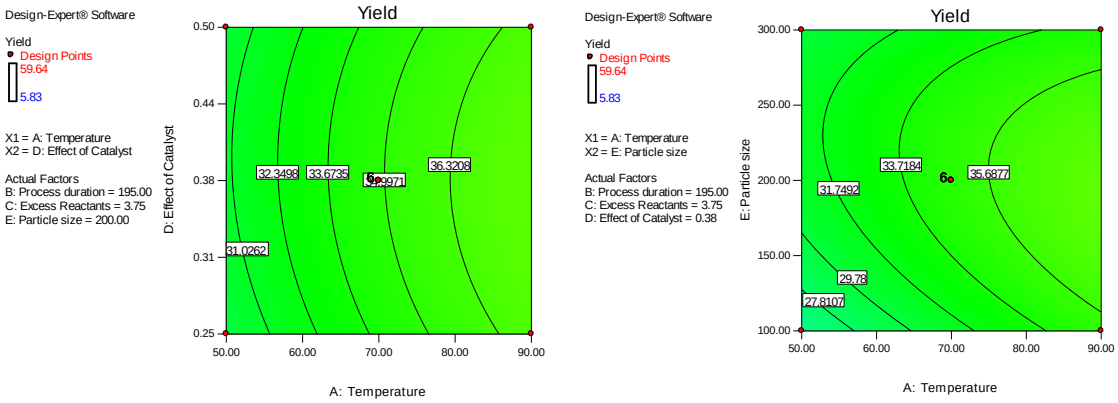

Fig. 15. The contour plots for the effect of catalyst against temperature and yield of BAC and The contour plots for particle size against temperature and yield of BAC

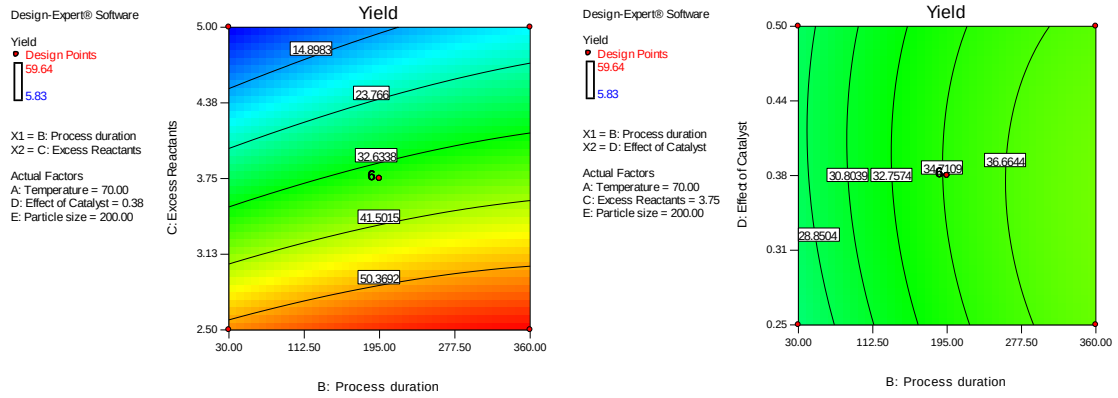

Fig. 16. The contour plots for excess reactants against process duration and yield of BAC and the contour plots for effect catalyst against process duration and yield of BAC

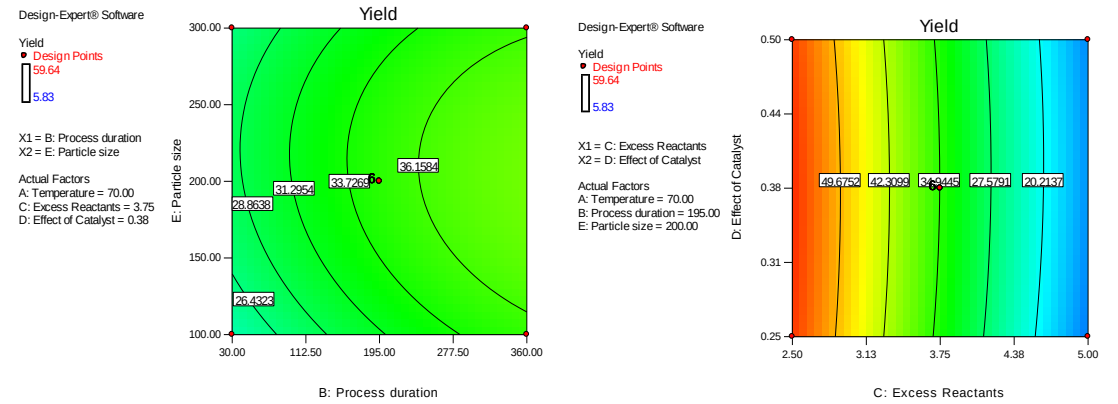

Fig. 17. The contour plots for particle size against process duration and yield of BAC and the contour plots for the effect of catalyst against excess reactants and yield of BAC

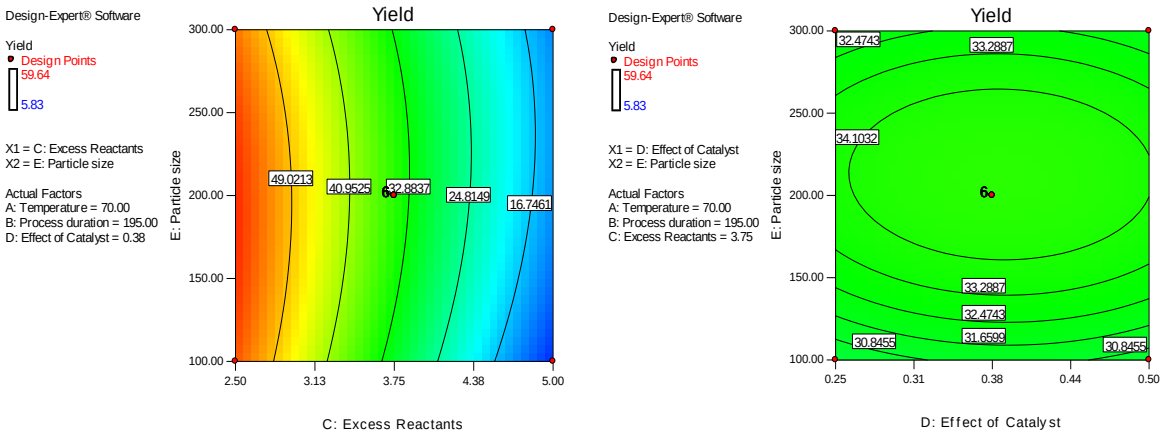

Fig. 18. The contour plots for particle size against excess reactants and yield of BAC and the contour plots for particle size against the effect of catalyst and yield of BAC

3.4.3 3-D plot for BAC

The 3 – Dimensional plots of the response surface model are shown in Figs. 19 and 20. The results showed that the optimum value of the conversion was 42 for the process variables studied, which are similar to results obtained by [25,35] and [37]. The excess reactants increase with process duration as the yield also increases. The response surface plots showed clear peaks, implying that the maximum values of the response were attributed to the factors in the design space. The three-dimensional surfaces provide useful information about the behaviour of the system within the experiment design, facilitate an examination of the effects of the experimental factors on the responses and contour plots between the factors [36,38,39,40] and [41].

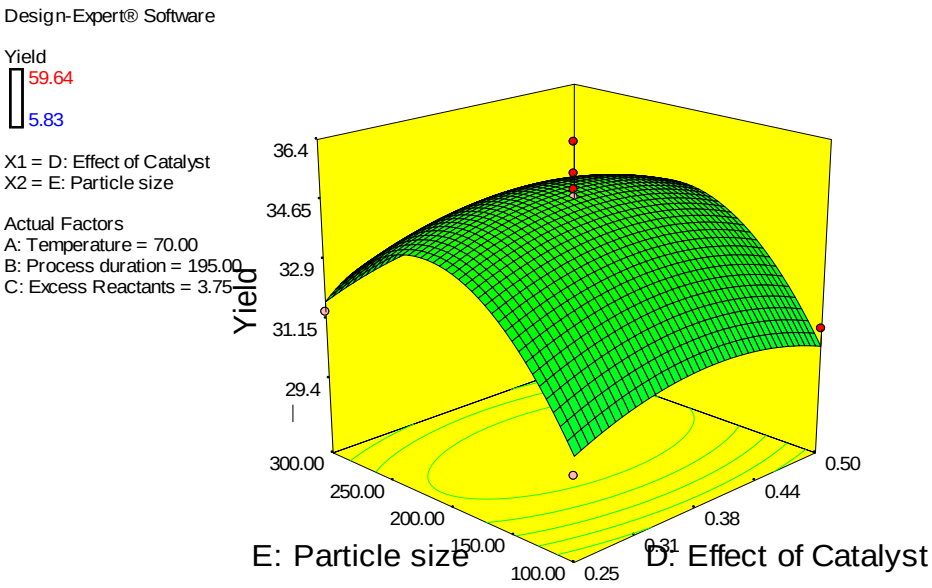

Fig. 19. The 3 - D Plotfor particle size against yield and effect of catalyst of BAC

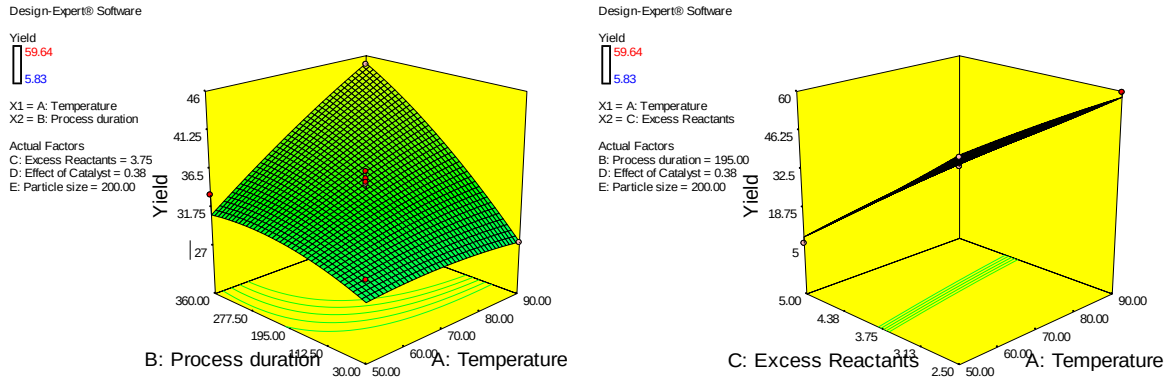

Fig. 20. The 3 - D Plotfor process duration against yield and temperature of BAC and 3 - D Plot for process duration against yield and temperature of BAC

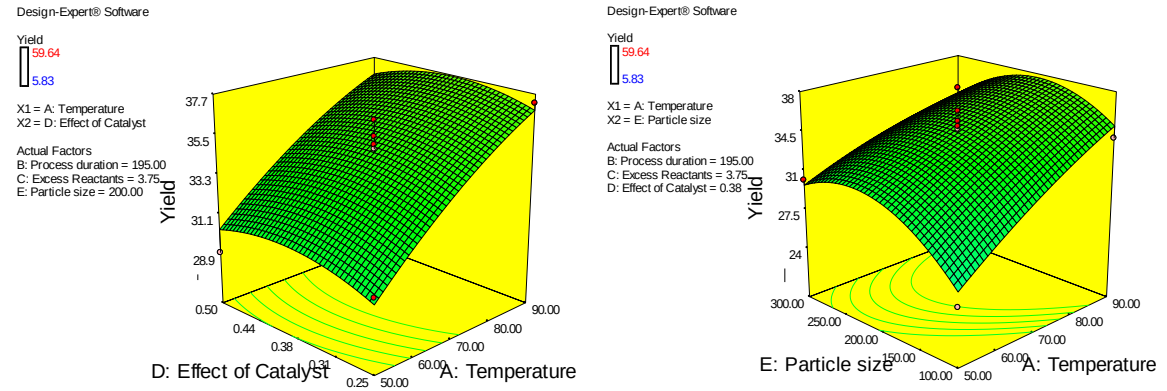

Fig. 21. The 3 - D Plotfor effect of catalyst against yield and temperature of BAC and 3 - D Plot for particle size against yield and temperature of BAC

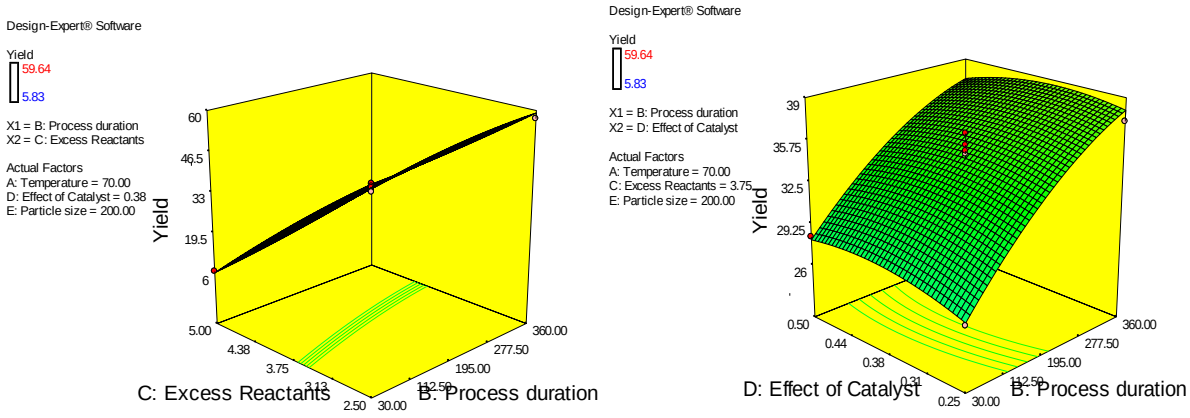

Fig. 22. The 3 - D Plot for excess reactants against process duration and temperature of BAC and The 3 - D Plot for the effect of catalyst against process duration and yield of BAC

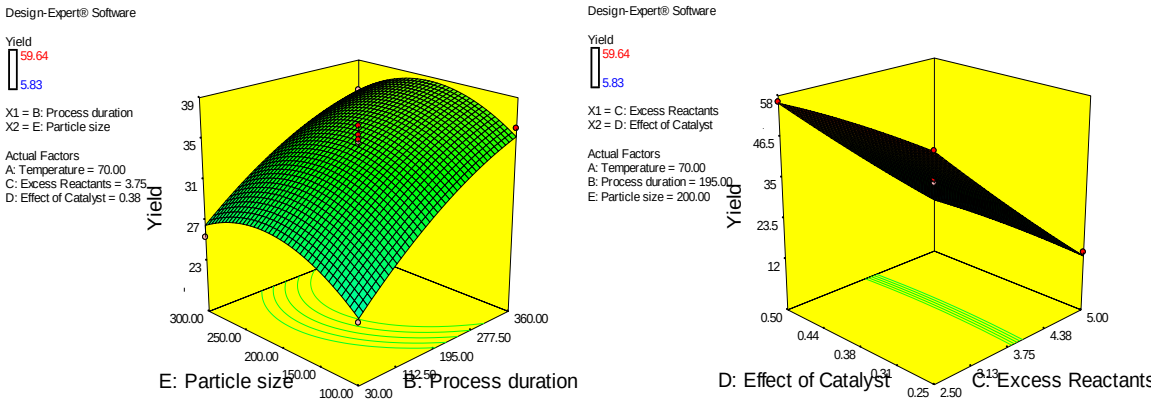

Fig. 23. The 3 - D Plot for particle size against process duration and yield of BAC and The 3 - D Plot for the effect of catalyst against yield and excess reactants of BAC

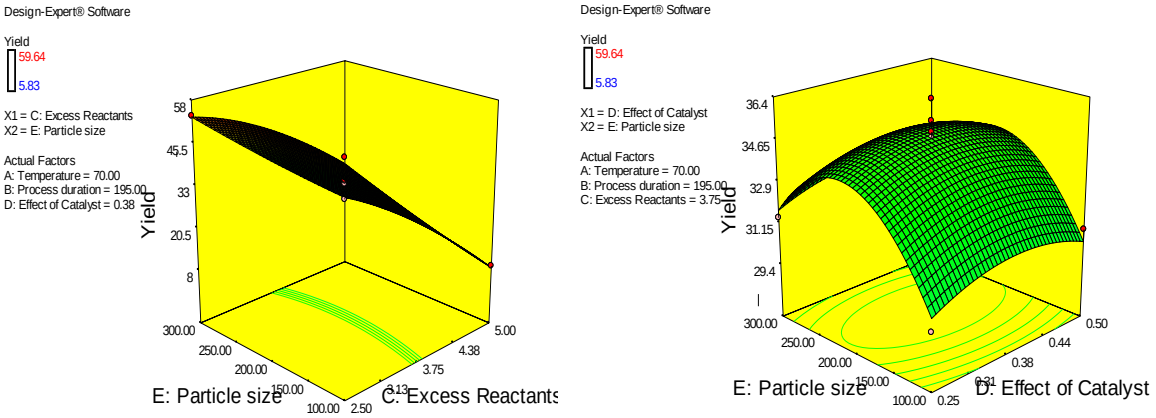

Fig. 24. The 3 - D Plot for particle size against yield and excess reactants of BAC and the 3 - D Plot for particle size against yield and effect of catalyst of BAC

4. CONCLUSIONS

The study presented the optimum conditions for acetic acid and ethanol esterification reaction using base activated Ngbo clay catalyst. The optimum conditions for esterification reaction for the process conditions of temperature, duration, amount of reactant, catalyst weight, and particle size was determined using Response Surface Methodology (RSM) approach. The optimum process conditions for the variables studied for a time, temperature, excess reactant, catalyst weight, and particle size were 359.99 min, 90^{o}C, 4.30ml, 0.50g, and 297.63 microns, respectively. The maximum predicted esterification yield was 30.3979. The XRF analysis showed that the clay was made of mainly SiO_2 and aluminum, while the XRD indicated quartz as the significant composition. The predicted and experimental values from the model showed less than 5% difference, thereby making the Box-Behnken design approach an efficient, effective, and reliable method for the esterification of acetic acid and ethanol using base-activated clay catalyst.

COMPETING INTERESTS

Authors have declared that no competing interests exist.

REFERENCES

1. Igbokwe PK, Ogbuagu JO. Effects of process parameters on the extraction of alumina from indigenous kaolinitic clay deposit. NJERD. 2003;2:2.

2. Shanmugan S, Viswanathan B, Varadarajan TK. Esterification by solid acid catalysts – a comparison. Journal of molecular catalysis A: Chemical. 2004;223: 143–147.
3. Ravendra Reddy C, Lyengar P, Nagendrappa G, Jai Prakash BS. Esterification of dicarboxylic acids to diesters over Mn^{+}-montmorillonite clay catalysts. Catalyst Letter. 2005;101:87–91.
4. Chen CC, Hayes KF. X-ray absorption spectroscopy investigation of aqueous Co(II) and Sr(II) sorption at clay-water interfaces. Geochim Cosmochim Acta. 1999;63:3205–3215.
5. Yadav GD, Thagathar MB. Esterification of maleic acid with ethanol over cation-exchange resin catalyst. React. Funct. Polym. 2002;52:99–110.
6. Zang Y, Ma L, Yang J. Kinetics of esterification of lactic acid with ethanol catalysed by cation-exchange resins. React. Funct. Polym. 2004;61:101–114.
7. Kirumakki SR, Nagaraju N, Chary KVR. Esterification of alcohols with acetic acid over zeolites Hβ, HY and HZSM5. Applied Catalysis A: General. 2006;299:185–192.
8. Kirumakki SR, Nagaraju N, Narayanan SA. Comparative esterification of benzyl alcohol with acetic acid over zeolites Hβ, HY and HZSM5. Applied Catalysis A: General. 2004;273:1–9.
9. Wu K, Chen Y. An efficient two-phase reaction of ethyl acetate production in modified ZSM- 5 zeolites. Applied Catalysis A: General. 2004;257:33–42.
10. Chu W, Yang X, Ye X, Wu Y. Vapour phase esterification catalysed by immobilized dodecatungstosilicic acid (SiW_{12}) on activated carbon. Applied Catalysis A: General. 1996;145:125–140.
11. Sepulvega JH, Yori JC, Vera CR. Repeated use of supported $H_3PW_{12}O_{40}$ catalysts in the liquid phase esterification of acetic acid with butanol. Applied Catalysis A: General. 2005;288:18–24.
12. Jermy BR, Pandurangan A. Catalytic application of Al-MCM-41 in the esterification of acetic acid with various alcohol. Applied Catalysis A: General. 2005;288:25–33.
13. Kirumakki SR, Nagaraju N, Chary KVR, Narayanan S. Kinetics of esterification of aromatic carboxylic acids over zeolites Hβ and HZSM5 using dimethyl carbonate. Applied Catalysis A: General. 2003;248: 161–167.
14. Nwabanne, Joseph T, Onu, Chijioke E. Nwankwoukwu, Okwudili C. Equilibrium, Kinetics and thermodynamics of the bleaching of palm oil using activated nando clay. Journal of Engineering Research and Reports. 2018;1(3):1-13.
DOI: 10.9734/JERR/2018/42699
15. Ajemba RO, Onukwuli OD. Process optimization of sulphuric acid leaching of alumina from Nteje clay using central composite rotatable design. International Journal of Multidisciplinary Sciences and Engineering. 2012;3(5):1–6.
16. Onu CE, Nwabanne JT. Application of response surface methodology in malachite green adsorption using Nteje clay. Open Journal of Chemical Engineering and Science. 2014;1(2):19–33.
17. Nwobasi Veronica Nnenna, Igbokwe Philomena K, Onu Chijioke Elijah. Removal of Methylene Blue Dye from Aqueous Solution Using Modified Ngbo Clay. Journal of Materials Science Research and Reviews. 2020;5(2):33-46.
18. Elijah CO, Nwabanne JT. Adsorption kinetics for Malachite green removal from aqueous solution using Nteje clay. Journal of Environment and Human. 2014;1(2): 133–150.
DOI: 10.15764/EH.2014.02015
19. Ezedinma Henry C, Nwabanne Jospeh T, E. Onu Chijioke E, Nwajinka Charles O. Optimum process parameters and thermal properties of moisture content reduction in water yam drying. Asian Journal of Chemical Sciences. 2021;9(4):44-54.
DOI:https://doi.org/10.9734/AJOCS/2021/v9i419080
20. Onyekwelu Ijeoma U, Nwabanne Jospeh T, Onu Chijioke E. Characterization and optimization of biodiesel produced from palm oil using acidified clay heterogeneous catalyst. Asian Journal of Applied Chemistry Research. 2021;8(3):9-23.
DOI:https://doi.org/10.9734/AJACR/2021/v8i330192
21. Onu CE, Igbokwe PK, Nwabanne JT, Ohale PE. ANFIS, ANN, and RSM modeling of moisture content reduction of

cocoyam slices. Journal of Food Processing and Preservation. 2021; e16032.

Available:https://doi.org/10.1111/jfpp.16032

22. Iheanacho Chamberlain Ositadinma, Nwabanne Joseph Tagbo, Onu Chijioke Elijah. Optimum process parameters for activated carbon production from rice husk for phenol adsorption. Current Journal of Applied Science and Technology. 2019; 36(6):1-11.

DOI: 10.9734/CJAST/2019/v36i630264

23. Igbokwe PK, Nwokolo SO, Ogbuagu JO. Catalytic esterification of stearic acid using a local kaolinitic clay mineral. NJERD. 2005;4:1.

24. Igbokwe PK, Olebunne FL. On the catalytic esterification of acetic acid with ethanol, using Nigerian montmorillonite clay: effect of reaction variables on catalyst efficiency. Journal of the University of Chemical Technology and Metallurgy. 2011;46(6): 389-394.

25. Igbokwe PK, Ugonabo VI, Obarandiku E, Ochili A. Characterization and use of catalyst produced from local clay resources. Journal of Applied Sciences (JAS). 2008;2:2.

26. Igbokwe PK, Olebunne FL, Nwakaudu MS. Effect of activation parameters on conversion in clay – catalysed esterification of acetic acid. International Journal of Basic and Applied Sciences. 2011;11(5):1–8.

27. Murat M, Amokrane A, Bastide JP, Montanaro L. Synthesis of zeolites from thermally activated kaolinite. Some observations on nucleation and growth. Clay Minerals. 1992;27(1):119.

28. Akolekar D, Chaffee A, Howe RF. The transformation of kaolin to low-silica X zeolite. Zeolites. 1997;19(5–6):359–365.

29. Demortier A, Golbeltz N, Letlieur JP, Duhayon C. Infrared evidence for the formation of an Intermediate compound, during the synthesis of Zeolite Na – A from metakaolin. International Journal of Inorganic Materials. 1999;1(2):129–134.

30. Tracy MMJ, Higgins JB. Collection of simulated XRD powder patterns of Zeolites. Fourth revised edition ed. 2001, Amsterdam Elsevier. 2001;379.

31. Evamako O. Yusuf, Efeovbokhan VE, Babalola R. Development and characterization of zeolite – A from Elefun kaolin. Journal of Physics Conference, Series. 2001;1378–032016.

32. Ramirez JH, Maidonaldo – Hedar FJ, Ferez AF, Moremo C, Costa CA. Madeira LM. Azo-dye orange II degradation by heterogeneous Fenton-like reaction using carbón – Fe catalysts. Applied Catalysis B: Environmental. 2007;75(3–4):312–323.

33. Ejikeme ME, Ejikeme PCN, Abalu BN. RSM optimization process for uptake of water from ethanol water solution using oxidized starch. Pacific Journal of Science and Technology. 2013;14(2):319-329.

34. Azargohar R, Dalai AK. Production of activated carbon from luscar char: Experimental and modeling studies. MicroporMesopor. Mater. 2005;85:219–225.

35. Igbokwe PK, Ugonabo VI, Iwegbu NA, Akachukwu PC, Olisa CJ. Kinetics of the catalytic esterification of propanol with ethanoic acid using catalyst obtained from Nigerian clays. Journal of the University of Chemical Technology and Metallurgy. 2008;345–348.

36. Anupam K, Dutta S, Bhattacharjee C, Datta S. Adsorption removal of chromium (VI) from aqueous solution over powdered activated carbon: Optimization through response surface methodology. Journal of Hazard. Mater. 2011;173:135–143.

37. Olebunne FL, Igbokwe PK, Onyelucheya OE, Osoka EC, Ekeke IC. Mechanistic modeling of clay-catalysed liquid-phase esterification of acetic acid. Journal of Emerging Trends in Engineering and Applied Sciences. 2011;2(4):631-635.

38. Panesar PS. Application of response surface methodology in the permeabilitation of yeast cells for lactose hydrolysis. Biochem. Eng. J. 2008;39:91–96.

39. Ahmad AA, Hameed BH. Effect of preparation conditions of activated carbon from bamboo waste for real textile waste water. Joural of Hazard Mater. 2010;173: 487–493.

40. Onu Chijioke Elijah, Igbokwe PK, Nwabanne JT, Nwanjinka OC, Ohale PE. Evaluation of Optimization techniques in predicting optimum moisture content

reduction in drying potatoe slices. Artificial intelligence in Agriculture. 2020;4:39-47. Available:http://doi.org/10.1016/j.aia.2020.04.001

41. Onu CE, Nwabanne JT, Ohale PE, Asadu CO. Comparative analysis of RSM, ANN and ANFIS and the mechanistic modelling in eriochrome black-T dye adsorption using modified clay. South African Journal of Chemical Engineering. 2021;36:24-42. Available:https://doi.org/10.1016/j.sajce.2020.12.003

Peer-review history:
The peer review history for this paper can be accessed here:
https://www.sdiarticle5.com/review-history/86652